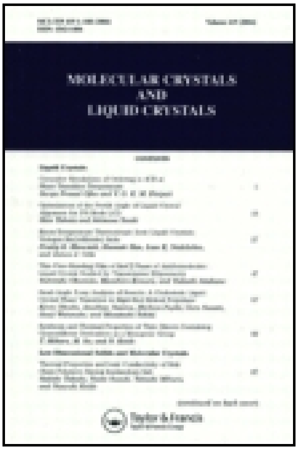

Molecular Crystals and Liquid Crystals
Publication details, including instructions for authors and subscription information:
http://www.tandfonline.com/loi/gmcl18

Diffraction Properties of Rectangular Phase Gratings in a Liquid Crystal Phase Modulator

M. W. Fritsch [a], C. Köhler [a], G. Haas [a], H. Wöhler [a] & D. A. Mlynski [a]

[a] Institut für Theoretische Elektrotechnik und Messtechnik, Universität Karlsruhe Kaiserstr, 12, 7500, Karlsruhe, Germany Phone: 49 721 6082620 Fax: 49 721 6082620

Version of record first published: 24 Sep 2006.

To cite this article: M. W. Fritsch, C. Köhler, G. Haas, H. Wöhler & D. A. Mlynski (1991): Diffraction Properties of Rectangular Phase Gratings in a Liquid Crystal Phase Modulator, Molecular Crystals and Liquid Crystals, 198:1, 1-14

To link to this article: http://dx.doi.org/10.1080/00268949108033378

Mol. Cryst. Liq. Cryst., 1991, Vol. 198, pp. 1–14
Reprints available directly from the publisher
Photocopying permitted by license only

Printed in the United States of America

Diffraction Properties of Rectangular Phase Gratings in a Liquid Crystal Phase Modulator

M. W. FRITSCH, C. KÖHLER, G. HAAS, H. WÖHLER and D. A. MLYNSKI

Institut für Theoretische Elektrotechnik und Messtechnik, Universität Karlsruhe Kaiserstr. 12, 7500 Karlsruhe, Phone: 49 721 6082620 Fax: 49 721 698025 Germany

(Received July 26, 1990)

The diffraction properties of rectangular phase gratings in a schlieren optical system are analysed. Those gratings are in a good approximation produced by liquid crystal control layers especially designed for phase modulation. In a first step, the dependence of the diffraction efficiency on the geometrical parameters of the control layer is investigated and optimum parameters for good efficiency and linearity are defined. In the second step, the influence of the schlieren optical system itself is analyzed, where the extension of the light source is taken into account. The optimum values for good contrast are evaluated. The problem of the tradeoff between contrast and intensity for high resolution can be solved by subdivision of the pixels which keeps the number of active addressing elements constant but produces a higher carrier frequency. The contrast can nearly be doubled in this case without loss of intensity.

Keywords: phase gratings, schlieren optical system, large screen projection, LC phase modulator

INTRODUCTION

Large screen projectors that use schlieren optical systems require phase modulating control layers. Usually, these layers are based on mechanically deformable materials like oil films or mirrors on elastomer carriers.[1,2,3] They modulate the phase by introducing optical path differences to the transmitted (or reflected) light due to different layer thickness. The phase differences cause a diffraction of the light into various orders as shown in Figure 1. With a lens these orders are focused in one plane where some orders are blocked, the rest is projected onto the screen. If the depth of the phase grating varies, the light distribution between the orders changes and so the intensity on the screen varies. Usually the dark field projection is used where the zeroth order is blocked so that the screen remains dark if the control layer is not addressed.

Alternatively to varying the thickness of a layer with a constant index of refraction, phase modulation can be achieved by changing the refractive index of the control layer with a constant thickness in the addressed area (Figure 2). This

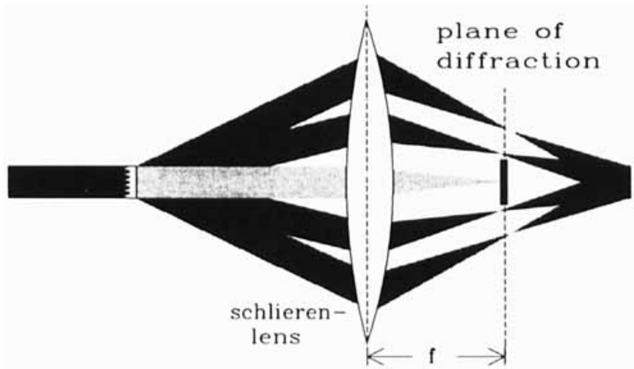

FIGURE 1 Principle of schlieren optical projection.

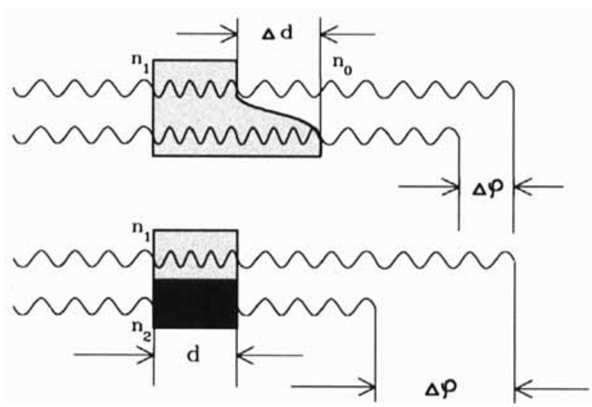

FIGURE 2 Phase differences produced by different layer thickness and constant index of refraction (a) or different index of refraction and constant thickness (b).

principle was proposed by Reference 4, where a liquid crystal layer was used as a medium with a controllable index of refraction. This control layer, however, used an untwisted nematic liquid crystal, so that only one polarization direction of the incident light was influenced. This means that 50% of the incident light are lost when conventional sheet polarizers are used. In References 5 and 6 a phase modulator was presented that uses twisted nematic liquid crystals as a control layer. Due to the symmetrical properties of the molecular orientation, all polarization directions of the incident light can be influenced so that no external polarizers are necessary. Thus the light efficiency is much better.

The efficiency and the contrast of the light valve depend on several parameters of both the light modulator itself and the schlieren optical system. The optical parameters of the liquid crystal layer were optimized in References 7 and 8 for maximum efficiency. This paper investigates the dependence on the geometrical parameters of both the control layer and the schlieren optical system with respect to image contrast and brightness. The spatial phase distribution that is produced by the liquid crystal is in good approximation rectangular, so the investigations are based on rectangular phase gratings.

THEORY

Schlieren optical systems can be described in terms of Fourier optics[9] and the basic schlieren optical system used e.g., in the G.E. light valve[2] or the Eidophor[1] has been analyzed by References 10–13. While the so far discussed optical control layers all produce nearly sinusoidal phase gratings[1–3] the liquid crystal produces a nearly rectangular phase grating. The mathematical description of the optical system as given in detail in References 10–13 remains valid, but the transfer properties of the modulator are different, so that the parameters of the whole transfer system change.

Figure 3 shows the basic schlieren optical system with the input and output filter bars, the schlieren lens and the modulator. The different planes that are important for the mathematical description are shown.

In this schlieren optical system, both lenses carry out a fourier transform if certain conditions for the focal length and the distances between the lenses are fulfilled. Then the signal transfer through the projection system can be described as follows:

The input signal is given by the input light that is modulated in phase by the control layer and contains no visible information. The first lens carries out a fourier

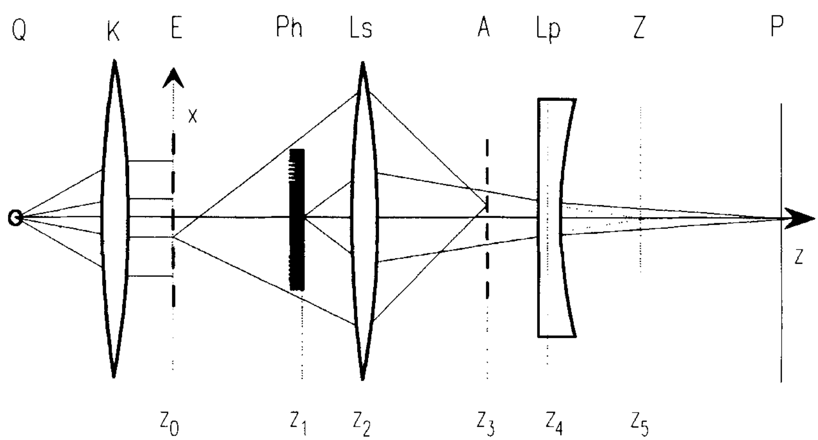

Q:	light source	A:	output bars
K:	condenser lens	L_P:	projection lens
E:	input bars	Z:	virtual image
Ph:	phase grating (control layer)	P:	screen
L_S:	schlieren lens		

FIGURE 3 Basic setup for a transmissive schlieren optical system with the relevant coordinate axes.

transform so that in the plane of the filter bars the spatial frequency spectrum of the input signal is present. The filter bars filter out certain parts of the spectrum, they act as a high pass (1 bar) or a band pass ($\gtrsim$ 1 bar). The second lens carries out another fourier transform to the output signal that is now amplitude modulated and so visible to the eye. So the following basic transfer system results:

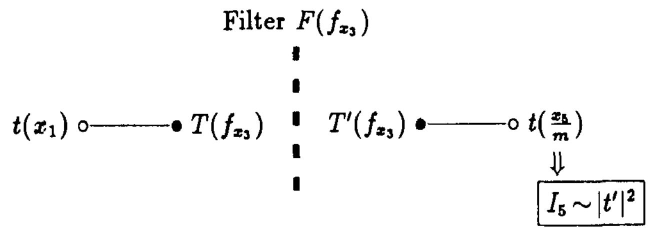

where $T(f_x)$ denotes the fourier transform of $t(x)$, m is a scaling factor. Although the light propagation in z-direction is a two-dimensional problem, the further discussion is limited to one coordinate (x), the parameters are assumed as constant in y-direction. So the elements are infinite in y and only a function of x.

RECTANGULAR PHASE GRATINGS

To calculate the diffraction properties of a rectangular phase grid, the parameters are defined as in Figure 4.

The width of a grating period is normalized to one. The width ratio k denotes

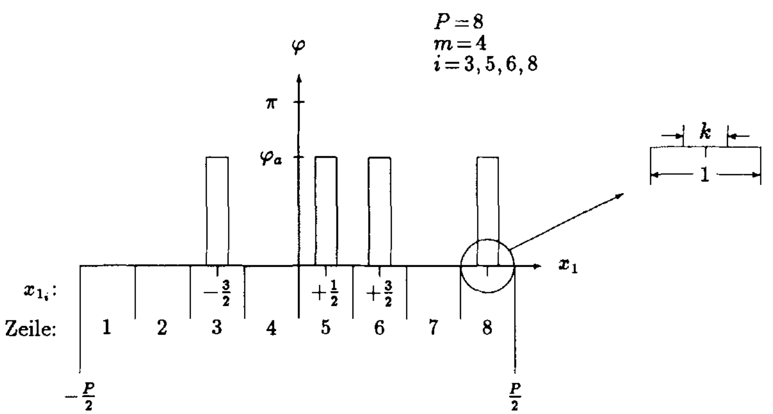

P:	width of the phase grating
m:	number of addressed lines
i ($i = 1, \ldots, m$):	line number
k:	width ration of one line $0 < k \leq 1$
φ_a:	phase of the addressed lines

FIGURE 4 Parameters in the rectangular phase grating.

the relative part of one period that is addressed. The phase delay φ_a controls the intensity of the m addressed lines. Although in general φ_a will be different for each line, it is assumed constant here for simplification. The phase grating is symmetrical with respect to zero $(-P/2\ \ +P/2)$. The center of an addressed line then has the coordinate x_{1_i}:

$$x_{1_i} = a_i - \frac{P+1}{2}$$

With these parameters the transmission function becomes:

$$t(x_1) = \begin{cases} e^{j\varphi_a} & ; \quad x_{1_i} - \frac{k}{2} \le x \le x_{1_i} + \frac{k}{2}; \\ e^{j0} = 1; & \quad else, \quad |x_1| \le \frac{P}{2} \end{cases} \tag{1}$$

From the transmission function the coefficients of the fourier series can be calculated as:

$$T_0 = \frac{1}{P} \int_{-\frac{P}{2}}^{\frac{P}{2}} t(x_1)dx_1 = \frac{1}{P} \int_{-\frac{P}{2}}^{\frac{P}{2}} \left(1 - \sum_{i=1}^{m} k(1-e^{j\varphi_a})\right) dx_1 = 1 - \frac{mk}{P}\left(1 - e^{j\varphi_a}\right) \tag{2}$$

which is the "DC-component," the only one that occurs in the non-addressed state. The other components for n, $m \neq 0$ are:

$$T_n = \frac{1}{P} \int_{-\frac{P}{2}}^{\frac{P}{2}} t(x_1) e^{-j2\pi f_n x_1} dx_1 = \frac{1}{P} \left[\int_{-\frac{P}{2}}^{\frac{P}{2}} e^{-j2\pi f_n x_1} dx_1 - \sum_{i=1}^{m} \int_{x_{1_i}-\frac{k}{2}}^{x_{1_i}+\frac{k}{2}} \left(1 - e^{j\varphi_a}\right) e^{-j2\pi f_n x_1} dx_1 \right] =$$

$$= -\frac{1}{j2\pi f_n P} \left[\underbrace{\left(e^{-j\pi f_n P} - e^{j\pi f_n P}\right)}_{=0(as\, f_n P = integer)} - \sum_{i=1}^{m} e^{-j2\pi f_n x_{1_i}} \left(e^{-jk\pi f_n} - e^{jk\pi f_n}\right) \right] (1 - e^{j\varphi_a}).$$

With $e^{-jk\pi f_n} - e^{jk\pi f_n} = -2j\sin(k\pi f_n)$ and $\mathrm{si}(x) = \frac{\sin(x)}{x}$:

$$T_n = -\frac{k}{P} \mathrm{si}^2(k\pi f_n) \left[\sum_{i=1}^{m} (e^{-j2\pi f_n x_{1_i}}) \right] (1 - e^{j\varphi_a}). \tag{3}$$

To calculate the image intensity, the mean square of the fourier coefficients must be calculated. With $|1 - e^{j\varphi_a}|^2 = 2(1 - \cos\varphi_a)$ the intensity distribution results.

$$I_n = \begin{cases} 1 - D(1 - \cos\varphi_a); & n = 0, \quad D = 2\frac{mk}{P}\left(1 - \frac{mk}{P}\right) \\ S_n(1 - \cos\varphi_a); & n, m \neq 0, \quad S_n = 2\left(\frac{k}{P}\right)^2 \mathrm{si}^2(k\pi f_n) \left| \sum_{i=1}^{m} (e^{-j2\pi f_n x_{1_i}}) \right|^2 \end{cases} \tag{4}$$

Equation 4 shows that for D, $S_n = 0$ the intensity I_0 (for the spatial frequency $f_n = 0$) equals one. This is the case for $m = 0$ (which represents a non-addressed phase grating) and corresponds to the undisturbed geometric imaging of the light source onto the filter bar.

In the ideal case with no light loss the sum of all orders is constant. So the diffracted intensity I_{dif} becomes:

$$\begin{aligned} I_{dif} &= 1 - I_0 = D(1 - \cos\varphi_a) \\ I_n &= S_n(1 - \cos\varphi_a); \quad n, m \neq 0 \end{aligned} \tag{5}$$

The parameter D is proportional to the diffracted intensity and S_n (n, $m \neq 0$) is proportional to the intensity of each different spatial frequency f_n.

Due to the dark field principle, the intensity I_0 is lost in any case. Depending on the filter parameters, a part of I_{dif} can reach the image plane.

So there are three important points[14]:

1. The expression $(1 - \cos\varphi_a)$, shown in Figure 5a, determines the addressing characteristics which is nearly linear with saturation for $\varphi_a = 0$ and $\varphi_a = \pi$. Addressing with $\varphi_a > \pi$ decreases the intensity. So maximum intensity is reached for $\varphi_a = \pi$.
2. The diffracted intensity I_{dif} should be proportional to the number of addressed lines m, so it is necessary that: $D \sim mk/P$ for $0 \leq mk/P \leq m$. Figure 6 shows D as a function of mk/P. As $m/P \leq 1$, k must be less than 0.5. The optimum value for k is $k \sim 0.4$, where the function is nearly linear in m and nearly maximum diffraction is reached (see the straight line $D = 0.48\, m/P$ in Figure 6 for comparison). For $k \leq 0.4$ the linearity is better, but the diffracted intensity is decreased. Maximum diffraction intensity is reached for $k = 0.5$,[6] but the linearity is much worse.
3. The relative intensity distribution in the spectrum is determined by D and S_n, it is independent of the absolute phase φ_a. This is different to phase modulators with a sinusoidal phase delay where the spectrum is given by Bessel-functions and so strongly depends on the value of the phase delay.

The intensity distribution is in general determined by the envelopping si^2-func-

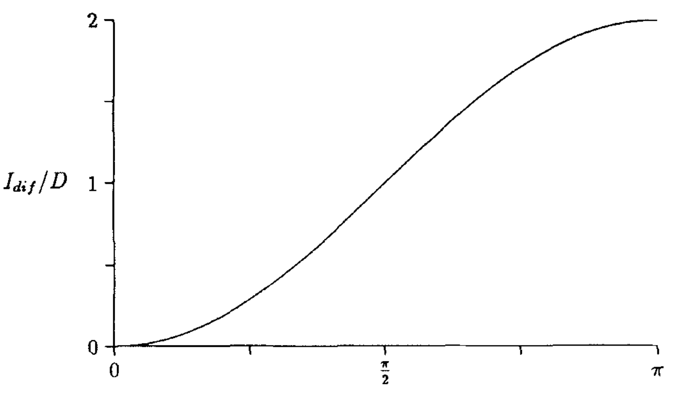

FIGURE 5 Voltage dependence of the phase modulator.

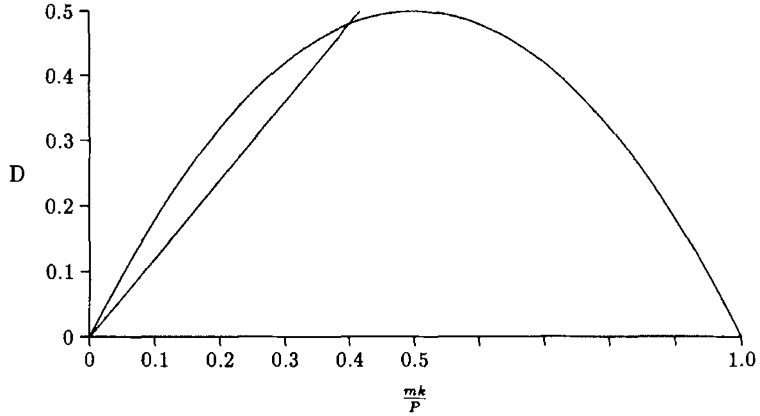

FIGURE 6 Diffraction parameter D as a function of the number of addressed lines and straight line for $k = 0.4$.

tion. The zeros of the envelopping function are at integers of kf_n, so their distance is proportional to $1/k$. So there are two important results for k ($k < 0.5$):

- For larger k more light is diffracted into higher orders $n \neq 0$.
- For smaller k the spectral bandwidth increases.

The information about the location of the addressed lines is contained in the complex coefficients S_n. This becomes visible only after the retransformation of the diffraction pattern, when the "DC"-component that contains no detail information has been filtered out of the transmission function $t(x_1)$.

SPATIAL FILTERING

The simple transfer system shown before is valid for the illumination by a point source. But real light sources must be considered as extended sources that are a

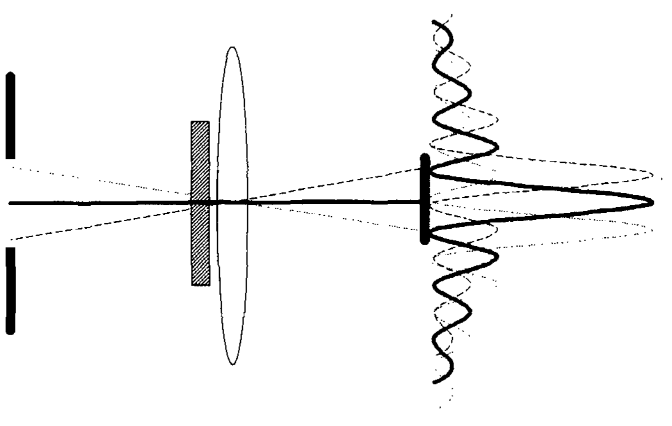

FIGURE 7 Position of the diffraction pattern for the different point sources of an extended source.

sum of single point sources that are incoherent to each other, but each source itself is spatially coherent (see e.g., Reference 10). Then the slits of the input bar system are filled with point sources that are imaged onto the output bars in the quiescent state. When the modulator is addressed, every point source produces a diffraction pattern whose location in the f_{x3}-plane depends on the location of the source in the x_0-plane (see Figure 7, where the width of the source is determined by the width of the input slit). The diffraction pattern is centered around the point onto which the point source is imaged. As the filter bars are fixed, the filter function depends on the location of the diffraction pattern. So a complete transfer step must be calculated for every point source, the resulting intensities of the sources are added up independently.

$$I_{5_{ges}}(x_5) = |\underline{A_5}|^2 \cdot \int_{-\infty}^{+\infty} \left| \int_{-\infty}^{+\infty} T'(f_{x_3} + \tfrac{Mx_0}{\lambda Q}) \cdot e^{-j2\pi(f_{x_3} \cdot \frac{x_5}{m})} df_{x_3} \right|^2 \cdot |L(x_0)|^2 \, dx_0 \quad (6)$$

where $1/\lambda Q$ is the scaling factor for the frequency axis and M the magnification of the source, $L(x_0)$ is the illumination on the x_0-axis, A the amplitude.

CONTRAST OPTIMIZATION

To calculate the frequency response of the projection system, the carrier grating is modulated with sine-shaped signals of different frequencies as shown in Figure 8. This modulation can be described as follows:

$$t(x_1) = 1 - \sum_{i=-\infty}^{\infty} \delta(x_1 - x_{1_i}) \cdot \left(1 - e^{j\varphi_a(\frac{1}{2} + \frac{1}{2}\sin 2\pi \frac{\nu}{p} x)}\right) * \sqcap_{\frac{k}{2}}(x_1), \quad (7)$$

$$\text{with } \sqcap_{\frac{k}{2}}(x_1) = \begin{cases} 1 & \text{for } -\frac{k}{2} \le x_1 \le \frac{k}{2} \\ 0 & \text{else.} \end{cases}$$

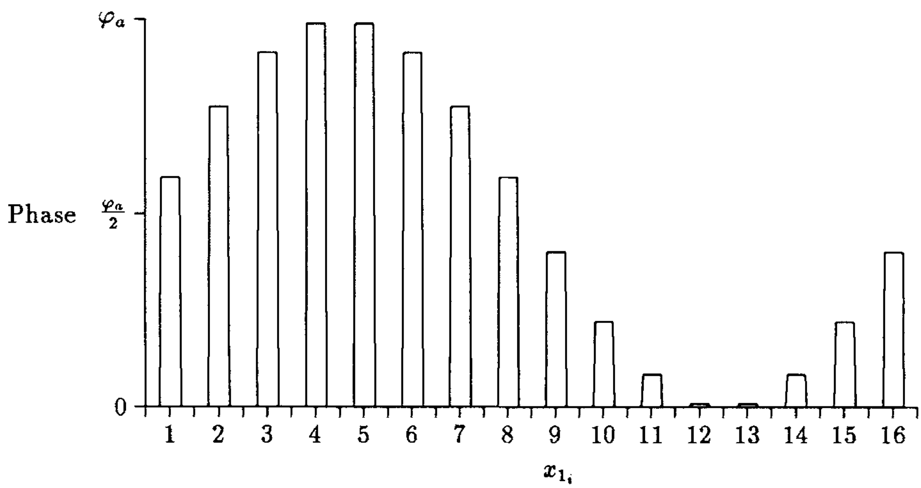

FIGURE 8 Phase grating modulated with a sinusoidal function.

The convolution with the "top-hat"-function leads to a broadening of the dirac impulses $\delta(x_{1_i})$ to the width k. The modulation function itself can be expressed in terms of Bessel-functions as[9]:

$$e^{j\frac{\varphi_a}{2}} \cdot e^{j\frac{\varphi_a}{2}\cdot\sin 2\pi\frac{\nu}{P}x_1} = e^{j\frac{\varphi_a}{2}} \cdot \sum_{m=-\infty}^{\infty} J_m\left(\frac{\varphi_a}{2}\right) \cdot e^{j2\pi\frac{\nu}{P}m\cdot x_1},$$

where $J_m(\varphi_\alpha)$ is the bessel-function of m-th order. Fourier transformation leads to:

$$T(f_{x_3}) = \delta(f_{x_3}) - k\,\mathrm{si}(k\pi f_{x_3}) \cdot \sum_{n=-\infty}^{\infty} \delta(f_{x_3} - nf_P) * \left[\delta(f_{x_3}) - e^{j\frac{\varphi_a}{2}} \cdot \sum_{m=-\infty}^{\infty} J_m\left(\frac{\varphi_a}{2}\right) \cdot \delta\left(f_{x_3} - \frac{\nu m}{P}\right)\right]. \quad (8)$$

So the modulation with a sine-wave leads to a convolution of the carrier frequency spectra with the modulation frequency spectra. That causes a widening of the carrier spectra which is proportional to the modulation frequency. Examples are shown in Figure 9. For lower modulation frequencies, the orders do not overlap (Figure 9a, b) so that they can easily separated by the filter. For higher frequencies the orders overlap so that they can no longer be separated (Figure 9c) so it is difficult to determine the optimum filter parameters.

Figure 10 shows the frequency response of the system for different widths of the central filter bar that blocks the zeroth order. The width of the passband is of minor importance if a certain width is guaranteed. For lower modulation frequencies, the contrast goes towards ∞ for all curves (in an ideal dark field). A smaller filter bar is optimum for low modulation frequencies, while for higher frequencies a wider bar gives a better contrast. On the other hand, a wider filter bar strongly reduces the intensity (~90% for 6/16, ~60% for 12/16) so that the width of the filter bar is a compromise between intensity and contrast if high resolution is desired.

The contrast is defined as the maximum of the output sine period divided by its minimum. Maximum and minimum are integrated over one period of the carrier grating (as that is the maximum resolution the observer should notice). The width of the light source is equal to the width of the passband in all cases. Equal overall light intensity is assumed for the input light independently of the filter parameters. The carrier frequency is 16, so a signal frequency of 3.8/16 means 3.8 periods of the modulating function per 16 carrier periods. The width ratio is chosen to $k = 13/32 = 0.406$.

Figure 11 shows the parameters for a system with 6 bars. The optimum filter width becomes higher for higher modulation frequencies as seen before, the influence of the passband is rather low. Only if the passband is so small that the second order is partly blocked, the contrast is reduced.

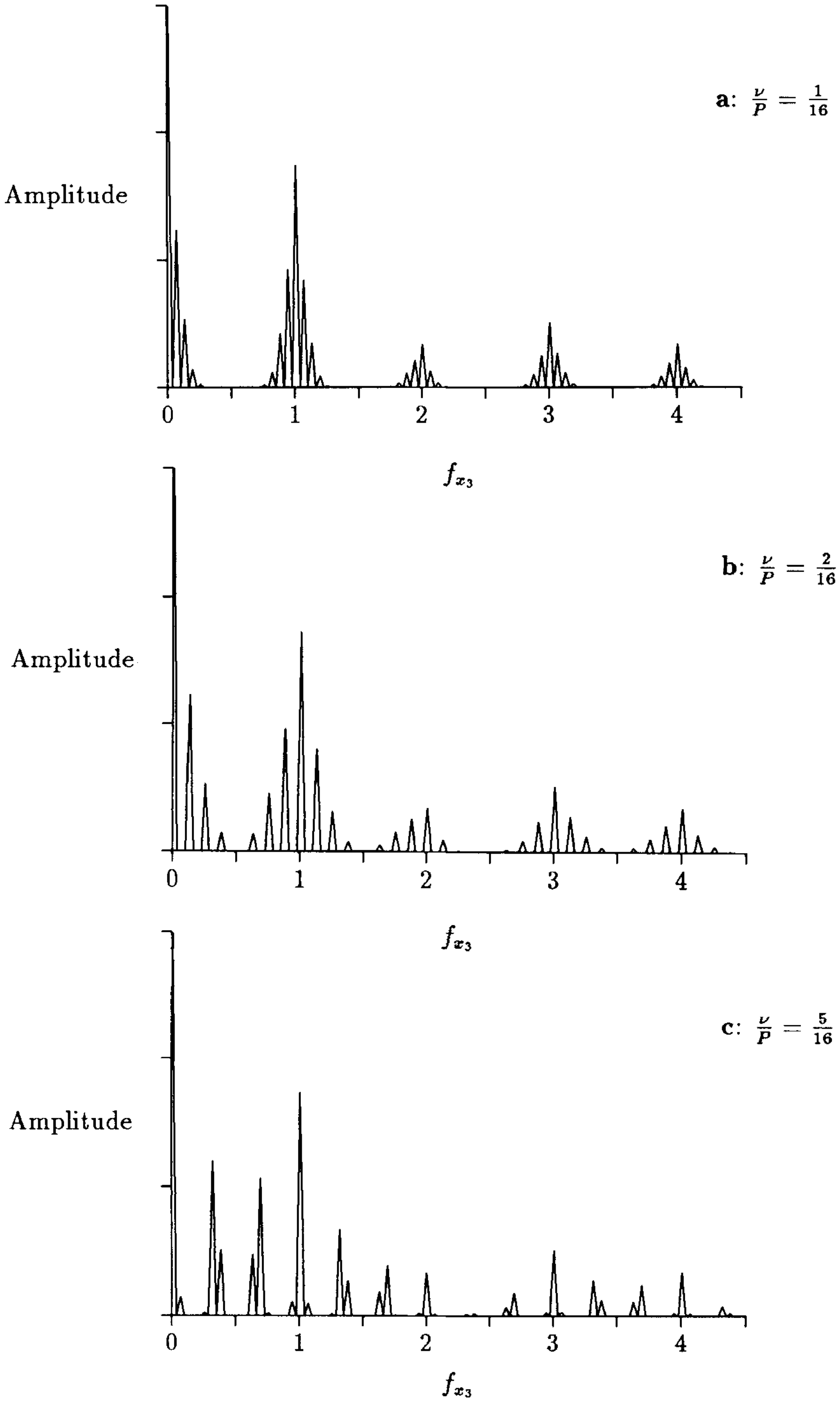

FIGURE 9 Diffraction pattern for sinusoidal modulation with low (a, b) and high (c) modulation frequency (the amplitudes are shown for better dynamics).

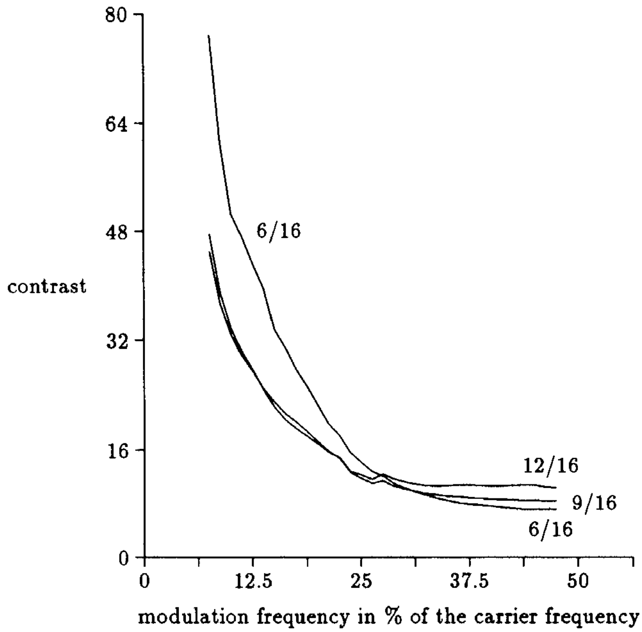

FIGURE 10 Contrast as a function of the modulation frequency.

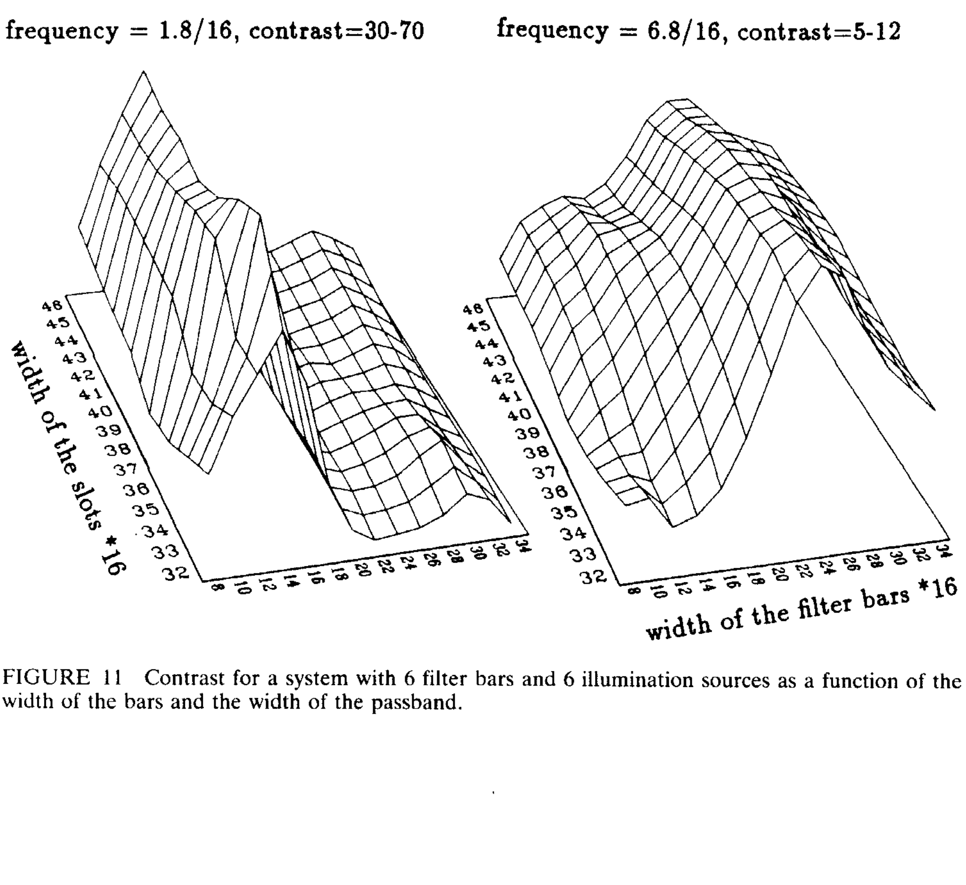

FIGURE 11 Contrast for a system with 6 filter bars and 6 illumination sources as a function of the width of the bars and the width of the passband.

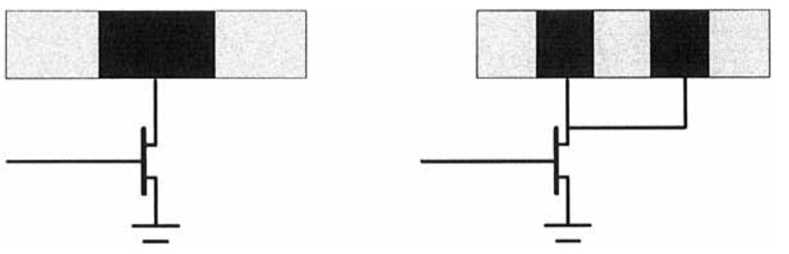

FIGURE 12 Subdivision of a pixel into two subpixels that are addressed by the same transistor.

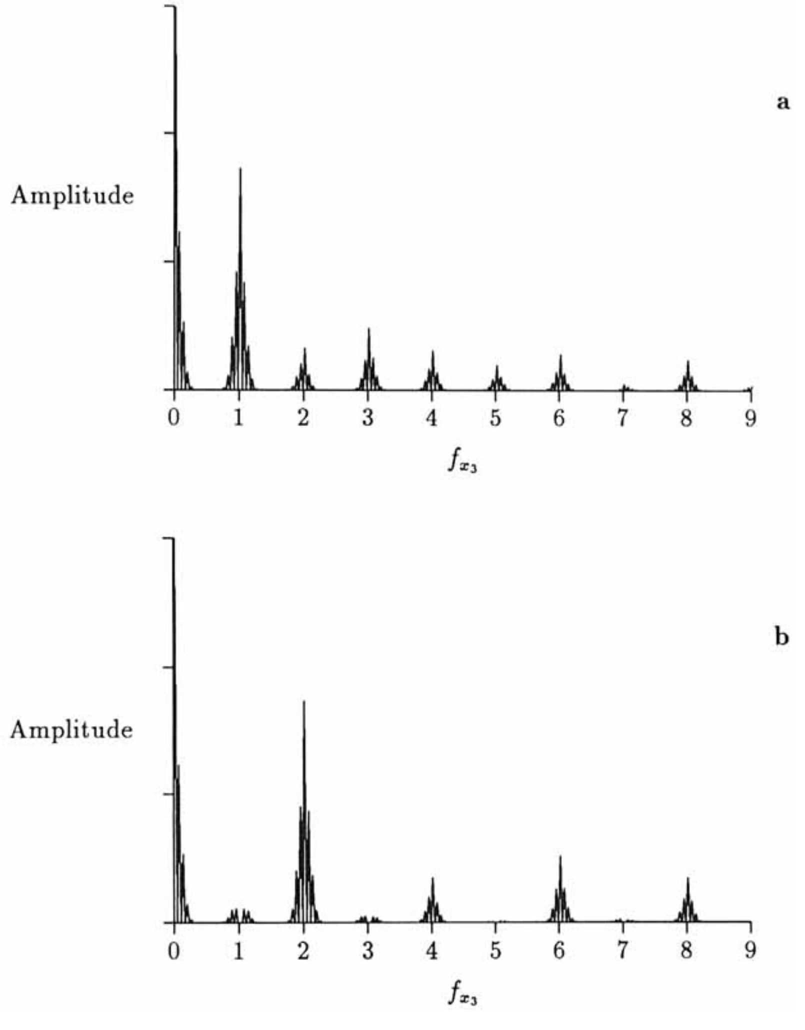

FIGURE 13 Spectra for sinusoidal modulation with one electrode per pixel (a) and subdivision of the pixel (b).

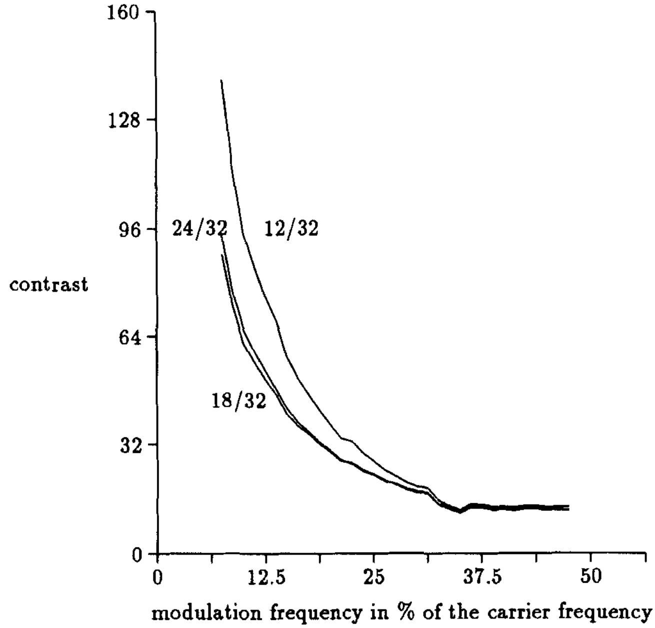

FIGURE 14 Contrast as a function of the modulation frequency for subdivided pixel.

DOUBLED CARRIER FREQUENCY

To avoid the overlapping of the orders, the carrier frequency can be doubled by dividing a pixel into two subpixels.[15] The two subpixels can be addressed by the same transistor so that the number of active elements remains constant (Figure 12). That means that every two adjacent lines have the same phase. The resulting spectra are shown for comparison in Figure 13. With the quasi doubled carrier frequency, every second carrier order becomes zero so that order separation is easier for higher modulation frequencies. Figure 14 shows the contrast under the same conditions as Figure 10 but with doubled carrier frequency. The contrast is higher than in Figure 10 and the optimum filter width does not change for higher modulation frequencies, hence the optimum can be clearly defined.

CONCLUSION

The diffraction properties of rectangular phase gratings in a schlieren optical system have been analyzed. Those gratings are in a good approximation produced by liquid crystal control layers especially designed for phase modulation. In a first step, the dependence of the diffraction efficiency on the geometrical parameters of the control layer was investigated and optimum parameters for good efficiency and linearity were defined. In the second step, the influence of the schlieren optical system itself was analyzed and the optimum values for good contrast could be evaluated. The problem of the tradeoff between contrast and intensity for high resolution can be solved by subdivision of the pixels which keeps the number of active addressing elements constant but produces a higher carrier frequency. The contrast can nearly be doubled in this case without loss of intensity.

References

1. F. Fischer and H. Thiemann, Theoretische Betrachtungen über ein neues Verfahren der Fernsehgrossprojektion. *Schweizer Archiv + Annales Suisses*, 7. Jahrgang (No. 1): pp. 1, 33, 305, 337 (1941).
2. W. E. Glenn. New color projection system. *J. Opt. Soc. Am.*, **48**(11), 841–843 (1958).
3. W. E. Glenn. Solid state driven deformable television light modulator. *SID Digest of Technical Papers 1987*, 72–74 (1987).
4. Y. Hori, K. Asai and M. Fukai. Field-Controllable Liquid-Crystal Phase Grating. *IEEE Transactions on Electron Devices*, Vol. ED-26 (No. 11): pp. 1734–1737, November 1979.
5. M. Fritsch, H. Wöhler, G. Haas and Mlynski. A Liquid-Crystal Phase Modulator for Large-Screen Projection. In *Proceedings of the 8th International Display Research Conference, San Diego, USA*, pp. 199–203 (1988).
6. M. Fritsch, H. Wöhler, G. Haas and D. A. Mlynski, "Liquid crystal phase modulator for large screen projection" IEEE Transaction on electron devices, vol. 36, No. 9, September 1989, p. 1882–1887.
7. M. W. Fritsch. *Schlierenoptische Grossprojektion mit Flüssigkristall-Phasenmodulator*. PhD thesis, Universität Karlsruhe, (1990).
8. M. Fritsch, H. Wöhler, G. Haas and D. A. Mlynski. Phase Modulation with Twisted Nematic Liquid Crystals for Schlieren Optical Projection Systems. In *10th International Display Research Conference*, Amsterdam, The Netherlands, (1990).
9. J. W. Goodman, *Introduction to Fourier Optics*, McGraw Hill, New York, (1968).
10. B. Kuhlow, "Spatial frequency filtering in an optical imaging system with an extended incoherent light source," *Applied Optics*, vol. 25, No. 14, July 1986, p. 2351–2356.
11. G. Tröller, H. J. Ehrke, B. Kuhlow, Th. Rosin, Th. Sinnig and R. Tepe, "Hochauflösende Darstellung farbiger Bewegtbilder," Heinrich Hertz Institute, Berlin, Final Report to the Project TK 140, (1985).
12. R. Tepe, "Beitrag zur Theorie von Einröhrenlichtventilverfahren in der Großbildprojektion," VDI Fortschrittsberichte Reihe 10, VDI-Verlag, Düsseldorf, (1987).
13. R. Kays, "Qualitätsverbesserung der Fernsehbildwiedergabe mit Eidophor Projektion" Dissertation Universität Dortmund, (1986).
14. C. Köhler, *Untersuchung der Beugungseigenschaften von Flüssigkristall-Phasengittern für schlierenoptische Projektionsverfahren*. Diplom thesis, Universität Karlsruhe, (1989).
15. R. Gerhard-Multhaupt, W. Brinker, H.-J. Ehrke, W.-D. Molzow, H. Roeder, Th. Rosin and R. Tepe. Viscoelastic spatial light modulators and schlieren-optical systems for HDTV projection displays. *SPIE*, Vol. 1255: pp. 1–10, (1990).